Solid State Communications 299 (2019) 113651

Contents lists available at ScienceDirect

Solid State Communications

journal homepage: www.elsevier.com/locate/ssc

Communication

Heavy-hole and light-hole excitons in nonlinear absorption spectra of colloidal nanoplatelets

A.M. Smirnov[a,c], V.N. Mantsevich[a,d,*], D.S. Smirnov[b], A.D. Golinskaya[a,d], M.V. Kozlova[a], B.M. Saidzhonov[e], V.S. Dneprovskii[a], R.B. Vasiliev[e]

[a] Moscow State University, Faculty of Physics, Chair of Semiconductors and Cruoelectronics, Moscow, 119991, Russia
[b] Ioffe Institute, St. Petersburg, 194021, Russia
[c] Kotelnikov Institute of Radio Engineering and Electronics, Russian Academy of Sciences, Moscow, 125009, Russia
[d] Moscow State University, Faculty of Physics, Quantum Technology Center, Moscow, 119991, Russia
[e] Moscow State University, Faculty of Materials Science, Moscow, 119991, Russia

ARTICLE INFO

Communicated by R. Merlin

Keywords:
Nanoplatelets
Exciton resonances
Pump-probe technique
Exciton interaction

ABSTRACT

We study the nonlinear optical response of CdSe/CdS nanoplatelets (NPLs) in the vicinity of heavy hole (hh) and light hole (lh) exciton resonances by means of the two color pump-probe technique. The population of hh and lh excitonic states leads to the decrease of the light absorption at both resonances under resonant excitation of one of them. Increase of the pump power leads to the saturation of the absorption. This effect allows us to estimate the exciton total lifetime.

1. Introduction

Colloidal semiconductor nanostructures represent an attractive alternative to the common MBE-grown nanosystems. Each of two types of low-dimensional structures consists of three families: 0D, 1D and 2D structures [1]. These families are called nanocrystals, nanorods, NPLs and quantum dots, quantum wires, quantum wells, in colloidal and epitaxially grown systems, respectively.

The most studied colloidal family is nanocrystals. The efficient methods were developed to control their size [2] and shape [3]. The strong quantum confinement allows one to tune the optical wavelength of nanocrystals in the wide range [4]. They were suggested for use in solar cells [5], bioimaging [6–8] and optoelectronic devices [9]. Ultimately they have recently become a part of commercially available devices [10].

Another family — 2D colloidal NPLs — also demonstrate a number of remarkable physical properties. First of all their optical resonance can be tuned due to the size quantization in one ($z \parallel [001]$) direction [11–14]. The binding energy of excitons in NPLs is of the order of a few hundreds of meV [15–17], which makes excitonic resonances in these systems visible at room temperature [18,19]. Moreover the surfaces of NPLs are atomically flat in contrast to quantum wells, so the excitonic lines are very sharp, of the order of a few tens of meV [20,21]. The NPLs are similar in a way to monolayers (MLs) of transition metal dichalcogenides [22,23], but have an important advantage of adjustable resonance wavelength [24,25].

All these outstanding properties of NPL triggered significant scientific interest in these structures [26–28]. Investigation of NPLs addresses mainly exciton recombination dynamics [29–31]. It was found that exciton-exciton interaction plays an important role [32,33], which suggests pronounced non-linear optical effects [34–37].

Here we study nonlinear transmission of CdSe/CdS NPLs with different shell thicknesses. We observe bleaching of excitonic transitions and saturation of exciton population in NPLs using the two color pump-probe technique.

The paper is organized as follows: In Sec. 2 we describe the procedure of colloidal synthesis of NPLs and their structure properties. Then in Sec. 3 we present experimental setup and experimental results, which are theoretically analyzed in Sec. 4. Comparison of theoretical model and experimental results allowed us to estimate parameters of exciton dynamics including average exciton lifetime and radiative recombination rate. The results are summarized in Sec. 5.

2. Synthesis and structural characterization of NPLs

We have studied core-shell NPLs based on thin population of CdSe NPLs with 463 nm lowest energy absorption band having 4.5 ML thickness accordingly to Ref. [38]. We grow 1 ML of CdS shell on each

* Corresponding author.
E-mail address: vmantsev@gmail.com (V.N. Mantsevich).

https://doi.org/10.1016/j.ssc.2019.113651
Received 22 February 2019; Received in revised form 23 April 2019; Accepted 4 June 2019
Available online 08 June 2019
0038-1098/ © 2019 Elsevier Ltd. All rights reserved.

basal plane of NPLs to synthesize 540 nm absorption core/shell nanoparticles (*CdSe/CdS*540) and 2 ML of CdS shell on each basal plane to get 582 nm absorption core/shell nanoparticles (*CdSe/CdS*582).

CdSe NPLs having 4.5 ML thickness were synthesized by the modified method adapted from Ref. [11]. In a typical synthesizes 0.5 mmol cadmium acetate, 0.2 mmol of oleic acid (OA) and 10 mL of octadecene (ODE) were introduced into a reaction flask. The mixture was degassed under magnetic stirring and argon flow at 180°C during 30 min. Then, the temperature was raised to 210°C and 0.2 mmol trioctylphosphine (TOP) Se solution was quickly injected into the mixture. The growth time of NPLs was 40 min at 210°C. The mixture was then cooled down to room temperature and 1 mL of OA was injected. As-synthesized CdSe NPLs were precipitated by adding an equal volume of acetone and centrifugation at 7000 rpm for 5 min and washed two times with acetone. Finally, NPLs precipitates were re-dispersed in 6 mL of hexane.

The synthesis of *CdSe/CdS* heterostructures was carried out by the method of low-temperature layer-by-layer deposition of shell material according to Ref. [39]. Briefly, 1 mL of a solution *CdSe* NPLs in hexane and 1 mL a freshly prepared 0.1 M solution of Na_2S in N-methylformamide (NMF) were mixed and shaken for 1 h. At the same time, a transfer of nanoparticles from the nonpolar hexane phase to the polar NMF phase was observed, which means the exchange of oleic ligands at the surface of NPLs by a ML of S^{2-}. The polar phase was rinsed several times with hexane and then the NPLs were precipitated by adding a mixture of acetonitrile and toluene (1 : 1 by volume) followed by centrifugation at 7000 rpm and redispersed in NMF. The precipitation-redispersion cycles were repeated two times to purify the residues from unreacted sulfur-ions. Then 1 mL of a solution 0.3 M of $Cd(OAc)_2{}^*2H_2O$ in NMF was added to the precipitate and left for 40 min to grow a CdS ML. The procedure described above corresponds to the synthesis of a single CdS ML. To obtain two MLs of CdS, this process was repeated two times. The synthesized NPLs were investigated experimentally in a liquid solution of methylformamide.

Low-resolution transmission electron microscopy (TEM) image of as-grown CdSe NPLs [Fig. 1(a)] demonstrates two-dimensional morphology. Rectangle platelets with lateral sizes about 30 × 100 nm rolled up into nanoscrolls. Fig. 1(b) presents typical image of CdSe NPLs after covering with 2 MLs of CdS. We found that initially rolled NPLs unfolded into flat nanostructures. As a result well-defined rectangle CdSe/CdS platelets with the same lateral sizes as CdSe NPLs were formed. The synthesized NPLs had zinc-blend crystal structure [12,29].

3. Experiment

We studied nonlinear optical properties of NPLs at room temperature using pump-probe technique. The simplified sketch of the experimental setup is depicted in Fig. 2. Pumping was realized by the mode-locked Nd^{3+}:$YAlO_3$ laser second harmonic (λ = 540 nm, pulse duration about 10 ns). As a probe we used a broadband photoluminescence radiation of the Coumarin-7 and Kiton Red dyes excited by the third harmonic (λ = 360 nm) of the pumping laser [40]. The temporal profiles of the pump and probe pulses are shown in Fig. 3(a). They were measured by a photomultiplier and oscilloscope (5 GHz) with the time resolution ~ 0.5 ns. Importantly, the durations of the pulses (~ 11 ns) exceeded by far the exciton generation, relaxation and recombination times. This allowed us to study the steady state conditions corresponding to the quasi-continuous excitation. This largely simplifies interpretation of the results and we also would like to mention that results of the time-resolved measurements can differ from the steady state measurements, which are the goal of this work.

The broad spectrum of the probe light is shown in Fig. 3(b), it covers the wavelengths from 480 to 600 nm by Coumarin-7 photoluminescence and from 590 to 660 nm by Kiton Red photoluminescence.

The transmission and absorption of the probe light was measured with spectral resolution using SpectraPro 2300*i* spectrometer with PIXIS 256 CCD-camera. The absorption spectra of *CdSe/CdS*540 and *CdSe/CdS*582 NPLs in 1 mm cell with methylformamide in the absence of pumping are shown in Fig. 4. The two pronounced peaks correspond to the hh and lh excitons [30]. The energies of these transitions are determined by the size quantization in direction perpendicular to NPLs. One can see, that the two peaks shift in *CdSe/CdS*582 NPLs with respect to *CdSe/CdS*540 NPLs because of the deeper penetration of the exciton wave function in CdS shell. The exciton binding energy in NPLs was calculated to be of the order of several hundreds of meV [16].

The wavelength of the pump laser is shown by the green arrow in Fig. 4. One can see that it corresponds to hh and lh excitonic transitions in *CdSe/CdS*540 and *CdSe/CdS*582 NPLs, respectively. As a result the pump light resonantly excited the corresponding excitonic states in the two studied samples.

The transmission spectra of the probe light for different pump powers are shown in Fig. 5. Here one can see the two dips corresponding again to hh-e and lh-e transitions. For the *CdSe/CdS*540 NPLs [panel (a)] dip in the transmission spectra corresponding to the hh-e transitions is more pronounced than the dip caused by the lh-e transition. In the case of the *CdSe/CdS*582 NPLs [panel (b)] the two dips in the transmission spectra can be clearly resolved. Increase of the pump power leads to the eventual disappearance of the dips.

We introduce the differential transmission at a given wavelength λ as

$$DT(\lambda) = \frac{T_I(\lambda) - T_0(\lambda)}{T_0(\lambda)}, \quad (1)$$

where $T_I(\lambda)$ is the transmission of the solution of colloidal NPLs at the

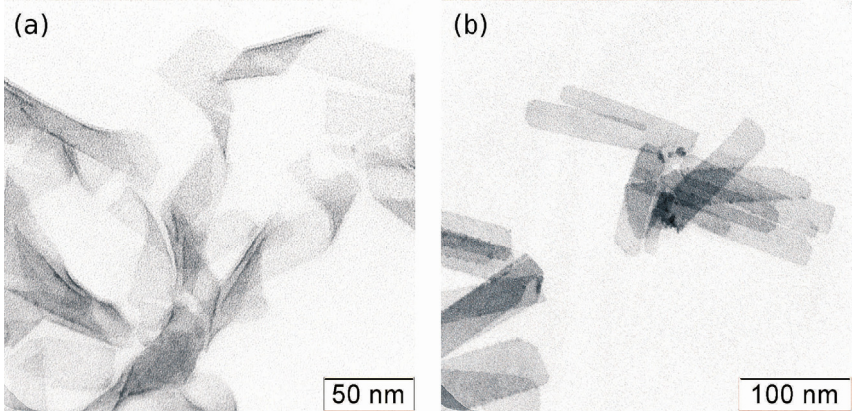

Fig. 1. Low-resolution transmission electron microscopy (TEM) overview images of as-synthesized *CdSe* NPLs (a) and *CdSe/CdS* NPLs with 2 ML of CdS on each of basal planes (b).

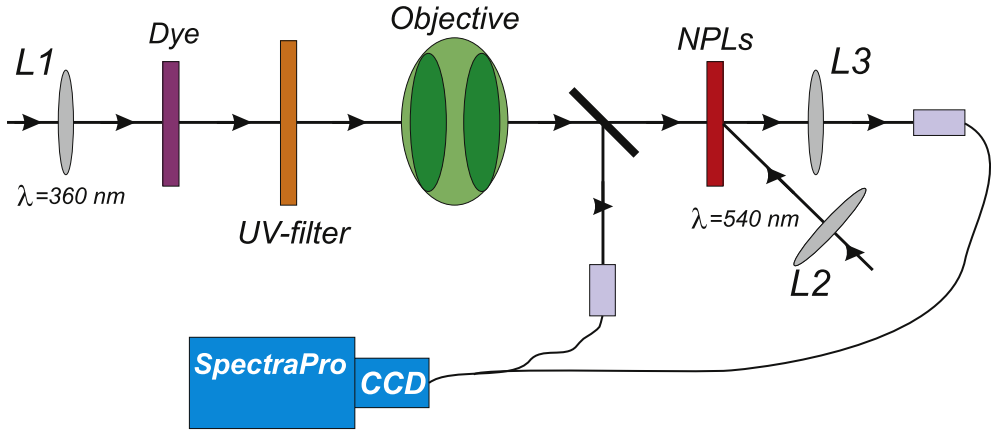

Fig. 2. Simplified sketch of the experimental setup.

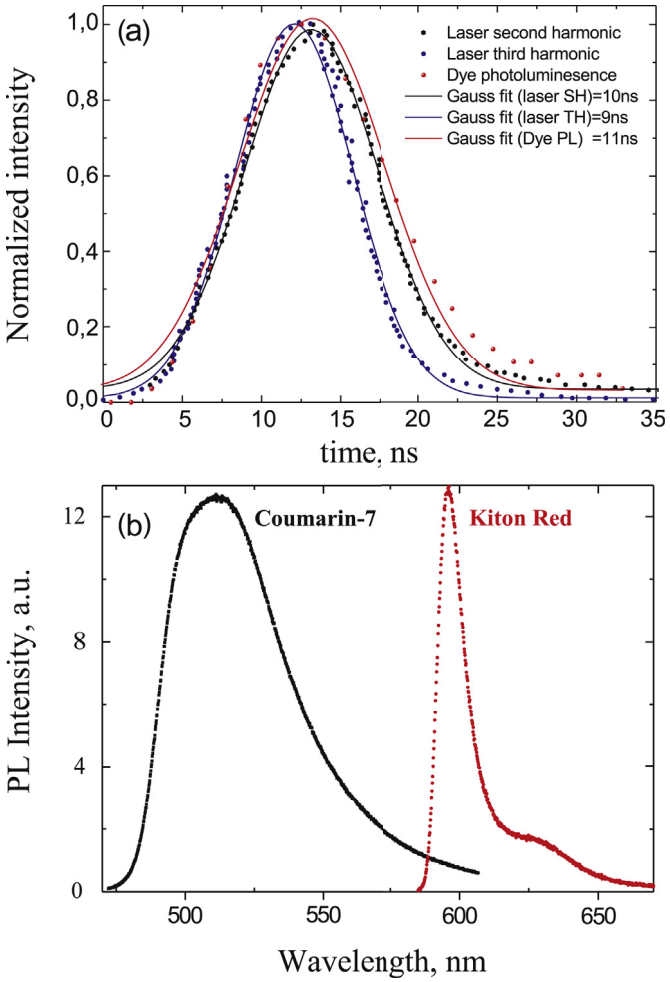

Fig. 3. (a) The temporal profiles of the pump pulse (red dots), the probe pulse (black dots) and the dyes excitation third harmonic pulse (blue dots). The curves show the corresponding Gaussian fits. (b) Spectra of the probe pulse, being the photoluminescence spectra of Coumarin-7 or Kiton Red dyes. (For interpretation of the references to color in this figure legend, the reader is referred to the Web version of this article.)

wavelength λ under pumping with intensity *I*. The differential transmission spectra are shown in Fig. 6. One can see, that the differential transmission gradually saturates.

In order to perform the detailed analysis we extract the areas under the differential transmission peaks corresponding to the hh-e and lh-e

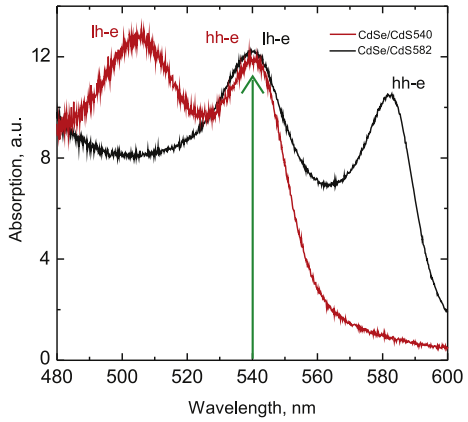

Fig. 4. Absorption spectra of colloidal solution of *CdSe/CdS*540 and *CdSe/CdS*582 NPLs. Green arrow shows the pump laser wavelength. (For interpretation of the references to color in this figure legend, the reader is referred to the Web version of this article.)

resonances as a function of the pump power. We find, that these dependencies for the both resonance are very similar, so in Fig. 7 we show the total area under the differential transmission curves. Here the saturation of the differential transmission for both samples is more evident.

4. Theory and discussion

The observed signal of the differential transmission can be produced by the three microscopic mechanisms [41] (i) phase space filling, (ii) screening of Coulomb interaction or (iii) broadening of the excitonic line. At the origin of all these mechanism is the exciton-exciton interaction. Since the areas of hh and lh peaks depend similarly on the pump power, we assume that each type of excitons equally affects the differential transmission at both resonances. Therefore the total differential transmission is proportional to the total number of excitons. A more detailed description of the experimental results in principle can be obtained releasing this assumption. Note, that the exciton fine structure [42] can be disregarded at room temperature [30].

Assuming that the excitons are pumped with the rate *G* and have the average lifetime τ the balance equation for the steady state reads

$$G\left(1-\frac{N}{N_s}\right)=\frac{N}{\tau}, \tag{2}$$

where we also introduced the saturation concentration of excitons N_s. From the solution of this equation we find that the differential transmission is proportional to

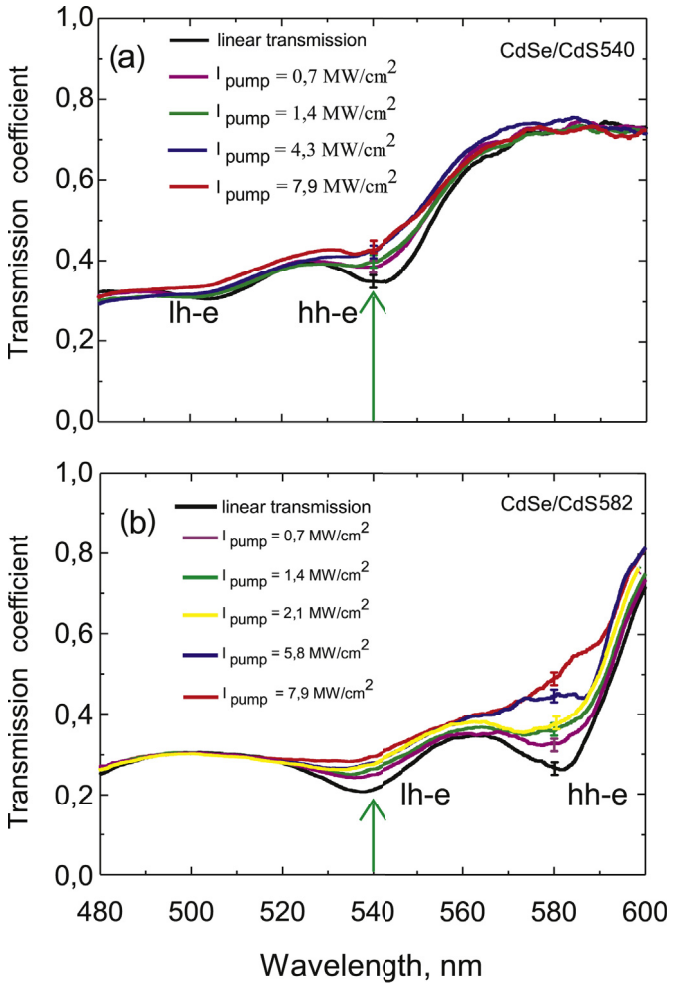

Fig. 5. Transmission spectra of (a) *CdSe/CdS*540 and (b) *CdSe/CdS*582 NPLs. The green arrow corresponds to the pump wavelength. The vertical bars show the characteristic statistical errors. (For interpretation of the references to color in this figure legend, the reader is referred to the Web version of this article.)

$$DT \propto N = \frac{G\tau}{1 + G\tau/N_s}. \tag{3}$$

We apply this expression to the description of the total area under the differential transmission, as shown by the curves in Fig. 7. From the fits we find the parameter

$$\frac{G\tau}{N_s P} = 0.54\,(0.62)\frac{\mathrm{cm}^2}{\mathrm{MW}}, \tag{4}$$

for *CdSe/CdS*540(582) NPLs. The inaccuracy of the fits in Fig. 7 is most probably related to the imprecise measurement of the differential transmission at small wavelengths, see Fig. 6(a).

The average exciton lifetime can be contributed by the charge trapping at the defect sites [30,36]. However this effect is suppressed due to the CdS shell, which strongly passivates defect states on the surface of the CdSe NPLs, and due to the high (room) temperature in our experiments. Both these factors were analyzed in Ref. [18], see also Ref. [43]. In what follows we will find the average exciton lifetime τ, which can be contributed by both radiative and nonradiative recombination of excitons.

The saturation concentration of excitons can be estimated as [44]

$$N_s = \frac{1}{\pi a_{\mathrm{eff}}^2}, \tag{5}$$

where a_{eff} is the effective exciton Bohr radius. The Coulomb interaction in NPLs is strongly modified due to the difference of the dielectric

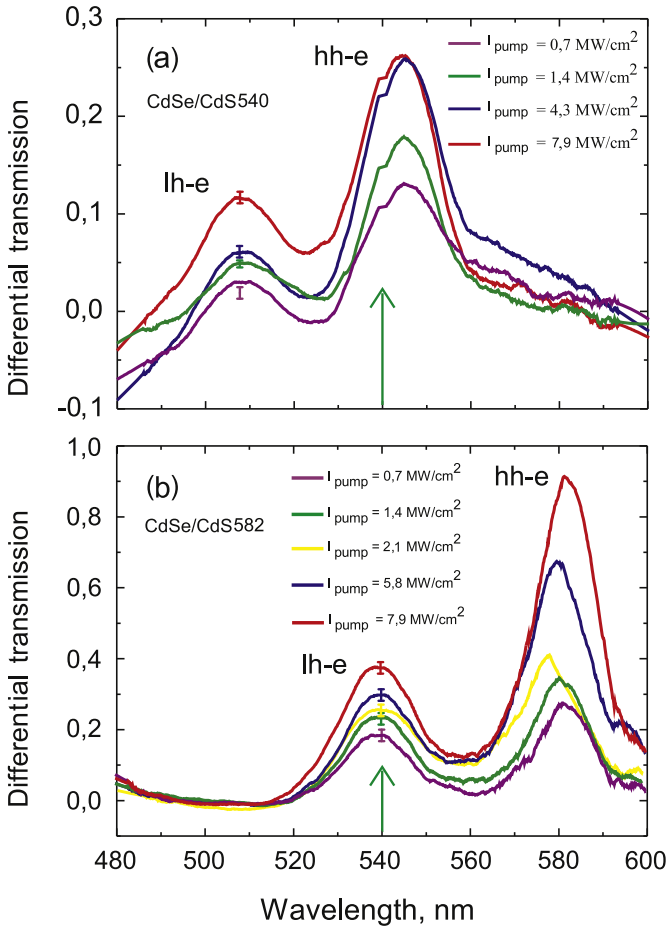

Fig. 6. The differential transmission spectra calculated after Eq. (1) for the different pump powers. Panel (a) corresponds to *CdSe/CdS*540 NPLs and panel (b) to *CdSe/CdS*582 NPLs. The vertical bars show the characteristic statistical errors.

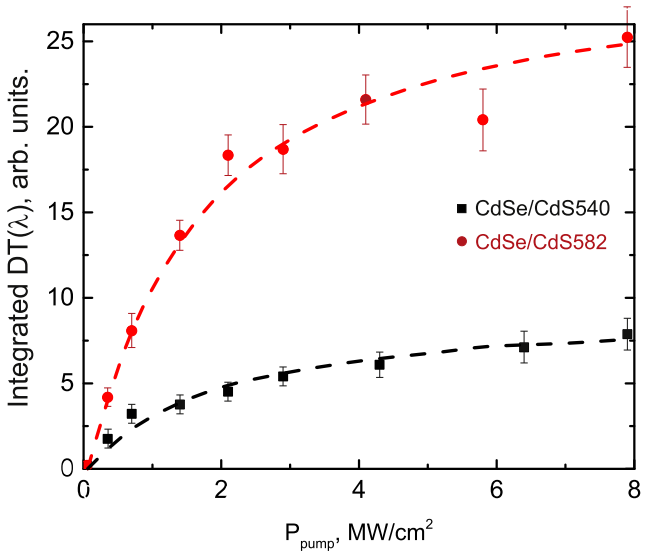

Fig. 7. Areas under the curves in Fig. 6 as a function of the pump intensity for *CdSe/CdS*540 NPLs (black dots) and *CdSe/CdS*582 NPLs (red dots). The curves show the fits after Eq. (3) with the parameter determined by Eq. (4). (For interpretation of the references to color in this figure legend, the reader is referred to the Web version of this article.)

constants of the NPLs, ε_0, and the solution ε_b [16,42]. As a result the electrostatic potential of the point charge q placed in the middle of the NPL at distance ρ also in the middle of the NPL is given by Ref. [45]

$$\phi(\rho) = \frac{q}{\varepsilon_0}\int_0^\infty J_0(k\rho)\frac{(\varepsilon+1)e^{kd}+\varepsilon-1}{(\varepsilon+1)e^{kd}-\varepsilon+1}\mathrm{d}k, \tag{6}$$

where $\varepsilon = \varepsilon_0/\varepsilon_b$, d is the thickness of the NPLs, and $J_0(x)$ is the Bessel function of the first kind. For the small excitons, their radius is given by Ref. [46]:

$$a_{\text{eff}} = \frac{\sqrt{a_B d}}{2}, \tag{7}$$

where a_B is the three dimensional exciton Bohr radius for the dielectric constant ε_0. This expression for the effective Bohr radius is valid in the limit $a_{\text{eff}} < \varepsilon d/2$. Using $a_B = 5.6$ nm [19] and $d = 3$ (4) nm for *CdSe/CdS*540(582) NPLs we find the effective radius $a_{\text{eff}} = 2$ (2.4) nm and the saturation concentration $N_s = 8$ (5.5) $\times 10^{12}$ cm^{-2}, respectively.

Further the exciton generation rate G is given by Ref. [1]

$$G = \frac{P}{\hbar\omega_0}\frac{2\Gamma_0}{\Gamma}, \tag{8}$$

where ω_0 is the pump frequency and $2\Gamma_0/\Gamma$ is the absorbance of the NPL with Γ_0 and Γ being, respectively, radiative and nonradiative damping rates. The exciton radiative recombination time τ_0 is given by Ref. [47]

$$\frac{1}{\tau_0} = 2\Gamma_0 = \frac{4q^3}{3\epsilon_b\hbar}|\mathcal{D}|^2, \tag{9}$$

where ϵ_b is the dielectric constant of the solution [48], $q = \sqrt{\epsilon_b}\omega_0/c$ is the light wavevector with c being the speed of light in vacuum, and

$$|\mathcal{D}|^2 = \frac{e^2E_pA}{\pi\omega_0^2 m_0 a_{\text{eff}}^2}. \tag{10}$$

Here e is the electron charge, E_P is the energy parameter measuring the Kane interband momentum matrix element, A is the area of NPL, m_0 is the free electron mass, and it is assumed that $Aq^2 \ll 1$. We note, that the imperfections of NPLs can lead to the exciton localization and effective reduction of A. However, we suppose the structure quality to be quite good and the room temperature to be high enough [18] to neglect this effect in the estimations. For the structure parameters $\hbar\omega_0 = 2.3$ eV, $A = 3000$ nm^2, $\varepsilon_b = 2$ ($\varepsilon_0 = 5.3$) and $E_P = 23$ eV [49], Eq. (9) yields $\hbar\Gamma_0 = 170$ and 120 μeV and the radiative lifetimes $\tau_0 = 1.9$ and 2.7 ps for *CdSe/CdS*540 and *CdSe/CdS*582 NPLs, respectively. The short radiative lifetime is related to the relatively large area of NPLs, see Eq. (10).

From Fig. 6 we estimate the exciton linewidth $\hbar\Gamma \approx 40$ meV. This ultimately allows us to find from Eq. (4) and the previous estimations the average exciton lifetime $\tau \sim 200$ ps for both samples. This is in a good agreement with Refs. [19,29,30,42]. The significant difference between τ_0 and τ is related to the fact that the radiative decay of excitons is possible only in the narrow radiative cone.

5. Conclusion

We studied experimentally nonlinear absorption and transmission of light in ensembles of CdSe/CdS NPLs. We used the two-color pump-probe technique with long pulse duration, which allowed us to study quasi steady state. We observed saturation of differential transmission. Theoretical analysis of this phenomenon allowed us to estimate the radiative recombination rate and the average exciton lifetime at room temperature. We believe, that investigation of nonlinear optical properties of colloidal NPLs performed in this paper will give a push to the development of optoelectronic devices operating at room temperature on the basis of colloidal NPLs.

Acknowledgements

We thank E. L. Ivchenko and A. A. Golovatenko for fruitful discussions and acknowledge the support by the Russian Science Foundation (Project 18-72-10002 - all experimental measurements) and the RFBR grant 16 − 29 − 11694 (samples synthesis). D.S.S. was partially supported by the RF President Grant No. MK-1576.2019.2, Russian Foundation for Basic Research (Grant No. 17-02-00383 and No. 17-52-16020) and the Basis Foundation.

References

[1] E.L. Ivchenko, Optical Spectroscopy of Semiconductor Nanostructures, Alpha Science Int., Harrow, UK, 2005.
[2] C.B. Murray, D.J. Norris, M.G. Bawendi, J. Am. Chem. Soc. 115 (1993) 8706.
[3] L. Manna, D.J. Milleron, A. Meisel, E.C. Scher, A.P. Alivisatos, Nat. Matter. 2 (2003) 382.
[4] Al. L. Efros, M. Rosen, Annu. Rev. Mater. Sci. 30 (2000) 475.
[5] C.-H.M. Chuang, P.R. Brown, V. Bulovic, M.G. Bawendi, Nat. Mater. 13 (2014) 796.
[6] B.A. Kairdolf, A.M. Smith, T.H. Stokes, M.D. Wang, A.N. Young, S. Nie, Annu. Rev. Anal. Chem. 6 (2013) 143.
[7] P.D. Howes, R. Chandrawati, M.M. Stevens, Science 346 (2014) 1247390.
[8] M.J. Bruchez, M. Moronne, P. Gin, S. Weiss, A.P. Alivisatos, Science 281 (1998) 2013.
[9] D.V. Talapin, J.S. Lee, M.V. Kovalenko, E.V. Shevchenko, Chem. Rev. 110 (2009) 389.
[10] T. Erdem, H.V. Demir, Nanophotonics 5 (2016) 74.
[11] S. Ithurria, B. Dubertret, J. Am. Chem. Soc. 130 (2008) 16504.
[12] S. Ithurria, M.D. Tessier, B. Mahler, R.P.S.M. Lobo, B. Dubertret, Al. L. Efros, Nat. Mater. 10 (2011) 936.
[13] W. Cho, S. Kim, I. Coropceanu, V. Srivastava, B.T. Diroll, A. Hazarika, I. Fedin, G. Galli, R.D. Schaller, D.V. Talapin, Chem. Matter 30 (2018) 6957.
[14] S. Christodoulou, J.I. Climente, J. Planelles, R. Brescia, M. Prato, B. Martin-Garcia, A.H. Khan, I. Moreels, Nano Lett. 18 (2018) 6248.
[15] M. Pelton, S. Ithurria, R.D. Schaller, D.S. Dolzhnikov, D.V. Talapin, Nano Lett. 12 (2012) 6158.
[16] R. Benchamekh, N.A. Gippius, J. Even, M.O. Nestoklon, J.-M. Jancu, S. Ithurria, B. Dubertret, Al. L. Efros, P. Voisin, Phys. Rev. B 89 (2014) 035307.
[17] A.W. Achtstein, A. Schliwa, A. Prudnikau, M. Hardzei, M.V. Artemyev, C. Thomsen, U. Woggon, Nano Lett. 12 (2012) 3151.
[18] M.D. Tessier, B. Mahler, B. Nadal, H. Heuclin, S. Pedetti, B. Dubertret, Nano Lett. 13 (2013) 3321.
[19] M.D. Tessier, C. Javaux, I. Maksimovic, V. Loriette, B. Dubertret, ACS Nano 6 (2012) 6751.
[20] B. Mahler, B. Nadal, C. Bouet, G. Patriarche, B. Dubertret, J. Am. Chem. Soc. 134 (2012) 18591.
[21] M. Nasilowski, B. Mahler, E. Lhuillier, S. Ithurria, B. Dubertret, Chem. Rev. 116 (2016) 10934.
[22] A. Kormanyos, G. Burkard, M. Gmitra, J. Fabian, V. Zclyomi, N.D. Drummond, V. Fal'ko, 2D Mater. 2 (2015) 022001.
[23] G. Wang, A. Chernikov, M.M. Glazov, T.F. Heinz, X. Marie, T. Amand, B. Urbaszek, Rev. Mod. Phys. 90 (2018) 021001.
[24] Z. Chen, B. Nadal, B. Mahler, H. Aubin, B. Dubertret, Adv. Funct. Mater. 24 (2014) 295.
[25] M.D. Tessier, P. Spinicelli, D. Dupont, G. Patriarche, S. Ithurria, B. Dubertret, Nano Lett. 14 (2014) 207.
[26] C. She, I. Fedin, D.S. Dolzhnikov, A. Demortiere, R.D. Schaller, M. Pelton, D.V. Talapin, D. Richard, Nano Lett. 14 (2014) 2772.
[27] B. Guzelturk, Y. Kelestemur, M. Olutas, S. Delikanli, H.V. Demir, ACS Nano 8 (2014) 6599.
[28] E.V. Shornikova, L. Biadala, D.R. Yakovlev, D. Feng, V.F. Sapega, N. Flipo, A.A. Golovatenko, M.A. Semina, A.V. Rodina, A.A. Mitioglu, M.V. Ballottin, P.C.M. Christianen, Y.G. Kusrayev, M. Nasilowski, B. Dubertret, M. Bayer, Nano Lett. 18 (2018) 373.
[29] L. Biadala, F. Liu, M.D. Tessier, D.R. Yakovlev, B. Dubertret, M. Bayer, Nano Lett. 14 (2014) 1134.
[30] L.T. Kunneman, J.M. Schins, S. Pedetti, H. Heuclin, F.C. Grozema, A.J. Houtepen, B. Dubertret, L.D.A. Siebbeles, Nano Lett. 14 (2014) 7039.
[31] M. Olutas, B. Guzelturk, Y. Kalestemur, A. Yeltik, S. Delikanli, H.V. Demir, ACS Nano 9 (2015) 5041.
[32] J.Q. Grim, S. Christodoulou, F. Di Stasio, R. Krahne, R. Cingolani, L. Manna, I. Moreels, Nat. Nanotechnol. 9 (2014) 891.
[33] E. Baghani, S.K. O'Leary, I. Fedin, D.V. Talapin, M. Pelton, J. Phys. Chem. Lett. 6 (2015) 1032.
[34] R. Scott, A.W. Achtstein, A. Prudnikau, A. Antanovich, S. Christodoulou, I. Moreels, M. Artemyev, U. Woggon, Nano Lett. 15 (2015) 4985.
[35] L.-B. Fang, W. Pan, S.-H. Zhong, W.-Z. Shen, Chin. Phys. Lett. 34 (2017) 098101.
[36] A.S. Selyukova, A.A. Isaev, A.G. Vitukhnovsky, V.L. Litvak, A.V. Katsaba, V.M. Korshunov, R.B. Vasiliev, Semiconductors 50 (2016) 947.
[37] J. Heckmann, R. Scott, A.V. Prudnikau, A. Antanovich, N. Owschimikow, M. Artemyev, J.I. Climente, U. Woggon, N.B. Grosse, A.W. Achtstein, Nano Lett. 17 (2017) 6321.

[38] A. Antanovich, A.W. Achtstein, A. Matsukovich, A. Prudnikau, P. Bhaskar, V. Gurin, M. Molinari, M. Artemyev, Nanoscale 9 (2017) 18042.
[39] S. Ithurria, D.V. Talapin, J. Am. Chem. Soc. 134 (2012) 18585.
[40] A.M. Smirnov, A.D. Golinskaya, K.V. Ezhova, M.V. Kozlova, V.N. Mantsevich, V.S. Dneprovskii, JETP 125 (2017) 890.
[41] A. Miller, P. Riblet, M. Mazilu, S. White, T.M. Holden, A.R. Cameron, P. Perozzo, J. Appl. Phys. 86 (1999) 3734.
[42] E.V. Shornikova, L. Biadala, D.R. Yakovlev, V.F. Sapega, Y.G. Kusrayev, A.A. Mitioglu, M.V. Ballottin, P.C.M. Christianen, V.V. Belykh, M.V. Kochiev, N.N. Sibeldin, A.A. Golovatenko, A.V. Rodina, N.A. Gippius, A. Kuntzmann, Ye Jiang, M. Nasilowski, B. Dubertret, M. Bayer, Nanoscale 10 (2018) 646.
[43] R.B. Vasiliev, D.N. Dirin, A.M. Gaskov, Russ. Chem. Rev. 80 (2011) 1139.
[44] S. Schmitt-Rink, D.S. Chemla, D.A.B. Miller, Phys. Rev. B 32 (1985) 6601.
[45] N.S. Rytova, Proc. MSU, Phys., Astron. 3 (1967) 30.
[46] L.V. Keldysh, JETP Lett. 29 (1979) 658.
[47] I.A. Yugova, M.M. Glazov, E.L. Ivchenko, Al. L. Efros, Phys. Rev. B 80 (2009) 104436.
[48] E.L. Ivchenko, V.P. Kochereshko, A.V. Platonov, D.R. Yakovlev, A. Waag, W. Ossau, G. Landwehr, Phys. Solid State 39 (1997) 1852.
[49] S. Shokhovets, O. Ambacher, B.K. Meyer, G. Gobsch, Phys. Rev. B 78 (2008) 035207.